The heavy noble gas composition of the depleted MORB mantle (DMM) and its implications for the preservation of heterogeneities in the mantle

Jonathan M. Tucker [a,*], Sujoy Mukhopadhyay [a], Jean-Guy Schilling [b]

[a] Department of Earth and Planetary Sciences, Harvard University, Cambridge, MA 02138, USA
[b] Graduate School of Oceanography, The University of Rhode Island, Narragansett, RI 02882, USA

ABSTRACT

To characterize the heavy noble gas composition of MORBs we present new He, Ne, Ar, and Xe abundances and isotopic compositions from the equatorial Mid-Atlantic Ridge. Both depleted MORBs nominally devoid of plume influence and more enriched MORBs thought to represent the influence of a HIMU mantle plume are present in close geographical proximity in this region. Ne–Ar–Xe isotopic compositions in individual step-crushes are correlated, which, along with significant radiogenic excesses, allows correction for shallow-level air contamination. Based on the relationship between the noble gases and the lithophile isotopes (Sr, Nd and Pb), the depleted MORB mantle has a $^{21}Ne/^{22}Ne$ between 0.0617 and 0.0646, $^{40}Ar/^{36}Ar$ ratio of $41,500 \pm 9000$ and $^{129}Xe/^{130}Xe$ ratio of 7.77 ± 0.06. On the other hand, the HIMU-type MORBs are characterized by far less radiogenic Ne, Ar and Xe isotopic compositions with mantle source $^{21}Ne/^{22}Ne$ between 0.0544 and 0.0610, and $^{40}Ar/^{36}Ar$ and $^{129}Xe/^{130}Xe$ ratios of $18,100 \pm 600$ and 7.21 ± 0.06, respectively. The observation of less nucleogenic $^{21}Ne/^{22}Ne$ in HIMU-type MORBs is similar to observations from HIMU ocean islands and requires the HIMU plume to be comprised of both recycled and primitive material. Within the depleted MORBs we observe He and Ne to be negatively correlated. The observation suggests that along the equatorial Atlantic the most depleted MORBs are related to normal MORBs through the addition of a small proportion of a HIMU plume component.

Our new Xe isotopic measurements demonstrate distinct $^{129}Xe/^{136}Xe$ ratios in the mantle sources of depleted MORBs, HIMU-type MORBs and the Iceland plume. While substantial injection of atmospheric Xe into these mantle sources is implied, the differences in Xe isotopic composition cannot result solely from recycling of air. Rather, they require that mantle plumes sample a reservoir less degassed than the depleted MORB mantle. This conclusion is consistent with a higher proportion of Pu- to U-derived fission Xe in Iceland and HIMU-type MORBs compared to the depleted MORBs. Overall, the Xe isotopic compositions imply that mantle plumes tap a reservoir that separated from the MORB source within the first 100 million years of Earth's history and that the two reservoirs have had limited direct mixing since then.

1. Introduction

Noble gas isotope ratios in mantle-derived rocks are powerful tools for understanding the structure and evolution of the Earth's mantle, the acquisition of terrestrial volatiles, and the exchange of material between the solid and fluid Earth (Allegre et al., 1987; Coltice et al., 2011; Gonnermann and Mukhopadhyay, 2009; Holland et al., 2009; Honda and McDougall, 1998; Marty, 1989; Marty and Tolstikhin, 1998; Ozima and Igarashi, 2000; Pepin, 1991; Porcelli and Wasserburg, 1995; Sarda et al., 1999; Trieloff and Kunz, 2005). Their low abundances, unreactive nature, and

preponderance of radiogenic and nonradiogenic (primordial) isotopes allow them to be ideal tracers of the degassing history of mantle reservoirs and the long-term interaction between these reservoirs. This is because small amounts of radiogenic ingrowth of noble gas daughter nuclides or admixtures of different material can dramatically alter noble gas isotope ratios, often in excess of other isotope systems by orders of magnitude.

Low ratios of the radiogenic to non-radiogenic noble gas nuclides (e.g. $^{21}Ne/^{22}Ne$, $^{40}Ar/^{36}Ar$, $^{129}Xe/^{130}Xe$) in ocean island basalts (OIB) compared to mid-ocean ridge basalts (MORB) are often used as evidence for a less degassed deep mantle and a more degassed, more processed upper mantle (e.g. Allegre et al., 1983, 1996; Gonnermann and Mukhopadhyay, 2009; Kurz et al., 1982; Porcelli and Wasserburg, 1995). The low ratios of $^{40}Ar/^{36}Ar$ and $^{129}Xe/^{130}Xe$ in OIBs have also been attributed to the recycling

of atmospheric noble gases (e.g. Holland and Ballentine, 2006; Trieloff and Kunz, 2005). However, Mukhopadhyay (2012) showed that the $^{40}Ar/^{36}Ar$ and $^{129}Xe/^{130}Xe$ in the mantle sources of the Iceland plume and the gas-rich MORB ("popping rock") from the north Atlantic (Kunz et al., 1998; Moreira et al., 1998) cannot be related solely through recycling of atmospheric noble gases; differences in the degree of mantle degassing are required to explain the observed Ar and Xe isotopic compositions.

The extent to which the noble gas composition of popping rock is representative of the depleted MORB mantle, however, is not clear. This is because the sample is highly enriched in trace elements ($La/Sm_N = 2.1$; Dosso et al., 1991, 1993) compared to the normal depleted MORBs (N-MORBs; $La/Sm_N \le 1$) that erupt along > 70% of the mid-ocean ridge system. Furthermore, recent work suggests that atmospheric noble gases are subducted into the mantle (Holland and Ballentine, 2006; Sumino et al., 2010; Kendrick et al., 2011) although the extent to which recycling affects the mantle noble gas budget is debated (Moreira and Raquin, 2007). Nonetheless, if the recycled component is distributed heterogeneously, large variations in MORB source Ar and Xe isotopic compositions would be expected. In this regard, Sarda et al. (1999) showed that maximum measured $^{40}Ar/^{36}Ar$ ratios in Atlantic MORBs were negatively correlated with $^{206}Pb/^{204}Pb$, such that the Pb isotopic evidence for recycled material was associated with maximum measured $^{40}Ar/^{36}Ar$ ratios that were closer in composition to the atmospheric $^{40}Ar/^{36}Ar$. The correlation suggests recycling of atmospheric Ar to the mantle via subducting plates. Burnard (1999), however, challenged Sarda et al.'s (1999) interpretation of Ar recycling as basalts with elevated $^{206}Pb/^{204}Pb$ are commonly found on topographic highs and those magmas would be more extensively degassed and more susceptible to atmospheric contamination, lowering their $^{40}Ar/^{36}Ar$ closer to the atmospheric ratio. Consequently, the extent to which noble gases are recycled, whether the recycled gases are distributed homogeneously throughout the mantle, and the average and variance of the Ne, Ar and Xe isotopic composition of the MORB source all remain poorly constrained.

To better characterize the variability in the noble gas composition of the MORB source we present new He, Ne, Ar, and Xe observations from the equatorial Mid-Atlantic Ridge. Basalts from the region of 5°N to 7°S span a range of compositions from among the most depleted MORBs ($La/Sm_N = 0.42$, $^{206}Pb/^{204}Pb = 17.64$) to among the most enriched ($La/Sm_N = 3.1$, $^{206}Pb/^{204}Pb = 20.09$). The enriched MORBs are thought to be related to the interaction of the HIMU-type (high μ, where μ is the U/Pb ratio) Sierra Leone plume with the Mid-Atlantic Ridge, whereas the depleted MORBs are devoid of plume influence (Hannigan et al., 2001; Schilling et al., 1994, 1995). Such large geochemical variations spanning nearly the entire range of Pb isotopic compositions seen in MORBs over a short geographical distance provide a unique opportunity to characterize the heavy noble gas variations in the MORB source, study the relationship between the noble gases and lithophile tracers, and thereby understand the relationship between the depleted MORBs and enriched MORBs. We use our new noble gas observations to address the following key questions:

1) What is the Ne, Ar, and Xe isotopic composition of depleted MORB mantle (DMM) and of the extremely depleted MORBs (D-DMM; Workman and Hart, 2005)?
2) What is the degree of heterogeneity in Ne, Ar and Xe in the MORB source and how were these heterogeneities created?
3) Are the HIMU-type MORBs also associated with primitive material as postulated for HIMU ocean islands (Day and Hilton, 2011; Parai et al., 2009)?

4) Are Ar and Xe being recycled back into the mantle, and if so, does this explain the differences in observed $^{40}Ar/^{36}Ar$ and $^{129}Xe/^{130}Xe$ ratios between MORBs and OIBs?

2. Methods

2.1. Samples

The samples used in this study were dredged from the equatorial Mid-Atlantic Ridge during the cruises of R/V Endeavor EN061 and R/V Conrad RC2806. They have been previously characterized for major elements, trace elements, Sr, Nd, and Pb isotopic compositions (Hannigan et al., 2001; Schilling et al., 1994, 1995). Some samples were reanalyzed for Pb isotopes (Agranier et al., 2005), and we use the newer measurements where applicable. For two of the samples, He isotopic compositions were previously determined by Graham et al. (1992b). We measured nine samples from between 5°N and 5°S for heavy noble gas abundances and isotope ratios. Four samples are depleted MORBs from between the Ascension and Chain fracture zones and five samples are HIMU-type MORBs from between 5°N and the Romanche fracture zone (Fig. 1).

Fresh basaltic glass for each sample was prepared by leaching in 5% HNO_3 and/or in 1% oxalic acid to remove minor surface alteration. Approximately 3–5 g of glass was loaded into a piston crusher and baked under vacuum at 90–100 °C for ~18 h to remove adsorbed gas. Glasses were step-crushed under vacuum, releasing the gas trapped in vesicles. Approximately 5–10 crushing steps were performed per sample, with each crushing step yielding a set of C, He, Ne, Ar, and Xe measurements.

2.2. Measurements

CO_2 concentrations were determined by manometry using 10 Torr MKS manometers directly attached to the crusher volume. Gases were purified by sequential exposure to hot and cold SAES getters and a small split of the gas was let into a quadrupole mass spectrometer to determine the Ar abundance and an approximate $^{40}Ar/^{36}Ar$ ratio. The noble gases were frozen onto a cryogenic cold trap and then sequentially released and let into the mass spectrometer. He, Ne, Ar and Xe abundances and isotopic compositions were measured on a Nu Noblesse noble gas mass spectrometer operating in multicollection mode. ^{20}Ne and ^{22}Ne were corrected for isobaric interferences from doubly-charged ^{40}Ar and
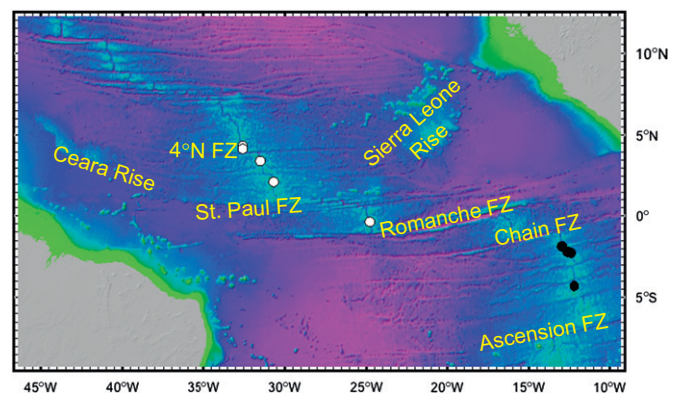

Fig. 1. Map of the Equatorial Atlantic showing the locations of the samples and the Sierra Leone Rise. The solid symbols between the Ascension and Chain fracture zones are the MORBs from the depleted group while the open symbols north of the Romanche fracture zone are the enriched HIMU-type MORBs.
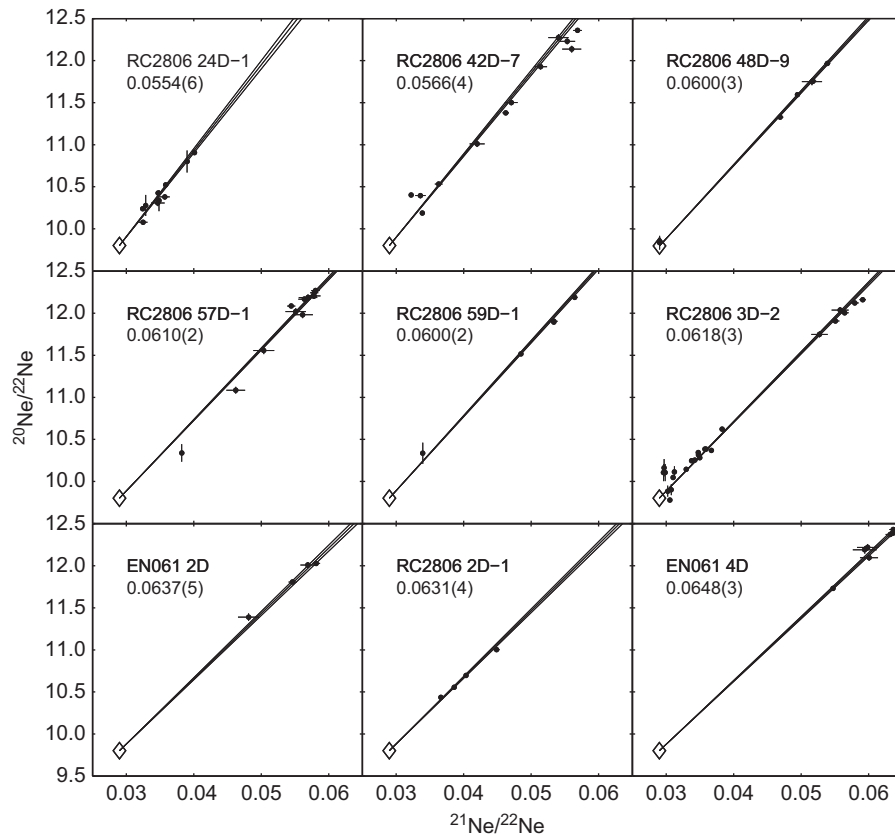
Fig. 2. Linear arrays in ^{21}Ne/^{22}Ne–^{20}Ne/^{22}Ne space for all nine samples that result from syn- to post-eruptive air contamination of bubbles containing mantle Ne. The mantle source ^{21}Ne/^{22}Ne was determined by x and y error-weighted least squares regression. Data points were translated such that the atmospheric composition was at (0,0). The y data were then scaled by the square root of the ratio of the variance in x to the variance in y so as to put x and y on the same scale and fitted with an equation of the form $y = mx$. The uncertainties in the slopes (shown by the 1σ error bands) were calculated using a Monte Carlo technique by randomly perturbing the data assuming normally distributed errors and refitting the slopes. The mantle value (^{21}Ne/^{22}Ne$_E$) was determined by extrapolation to ^{20}Ne/^{22}Ne of 12.5. The extrapolated values and their uncertainties are given in each panel.

^{44}CO$_2$ respectively. The Ar^{++}/Ar$^+$ was 0.061 ± 0.002 and the CO$_2^{++}$/CO$_2^+$ was 0.0055 ± 0.0005. For the Ar measurements, depending upon the Ar abundance and approximate isotope ratio previously determined by the quadrupole mass spectrometer, a fraction of the gas was let into the mass spectrometer for more precise isotope ratio determination. Mass spectrometric procedure is described in Mukhopadhyay (2012). Typical procedural blanks for ^{4}He, ^{22}Ne, ^{36}Ar and ^{130}Xe prior to the starting crush were 2×10^{-11}, 5.7×10^{-14}, 3.7×10^{-13}, and 1.8×10^{-16} cc, respectively. Blank levels were stable or decreasing during the course of crushing, with the exception of He, which increased by up to a factor of 2–4. Ne, Ar, and Xe blank isotopic ratios were statistically indistinguishable from atmosphere, and because the sample gases themselves are a mixture of mantle and shallow-level air contamination, no blank corrections were applied to the step–crushes. Mass discrimination for He was determined using the HH3 standard with a ^{3}He/^{4}He ratio of 8.81 R_A (Gayer et al., 2008) and for Ne, Ar, and Xe using air standards. Instrumental drift in sensitivity and mass discrimination was monitored through sample-standard bracketing with additional standards run overnight. Abundances and isotope ratios are reported in Tables S1 and S2.

2.3. Determination of mantle source isotopic ratios

For Ne, Ar, and Xe, each crushing step samples a population of bubbles reflecting variable mixtures of mantle-derived noble gases and syn- to post-eruptive atmospheric contaminants. As a result, noble gas compositions of bubbles define a mixing array

that lies between the atmospheric end-member and the mantle end-member. In ^{20}Ne/^{22}Ne vs. ^{21}Ne/^{22}Ne space, the array is linear, while in Ne–Ar, Ne–Xe, or Ar–Xe space the array can be described by a hyperbolic mixing equation. Assuming the ^{20}Ne/^{22}Ne ratio of the MORB source mantle is 12.5 (see Section 3.3), a particular isotope ratio (e.g. ^{21}Ne/^{22}Ne, ^{40}Ar/^{36}Ar) can be regressed against ^{20}Ne/^{22}Ne and extrapolated to a ^{20}Ne/^{22}Ne of 12.5 to determine the mantle source value.

The mantle source ^{21}Ne/^{22}Ne was determined by x and y error-weighted least squares regression forced through the atmospheric composition ($y = mx$) and extrapolation to ^{20}Ne/^{22}Ne of 12.5 (Fig. 2). Ar and Xe isotope ratios for the mantle source were determined using an iterative nonlinear least squares hyperbolic fit constrained to go through the atmospheric composition ($Ax + Bxy + Cy = 0$). We present Ar and Xe mantle source values for two samples that show well-defined hyperbolic mixing arrays. Such hyperbolic arrays are likely to reflect either a single atmospheric contaminant or two elementally-fractionated atmospheric contaminants present in nearly fixed proportions. We denote all extrapolated mantle source isotope ratios extrapolated to a ^{20}Ne/^{22}Ne ratio of 12.5 with a subscript "E".

2.4. Deconvolution of Pu- and U-derived fission Xe

To deconvolve U- from Pu-derived fissiogenic Xe, four mantle source Xe isotope ratios were used (^{130,131,134,136}Xe/^{132}Xe$_E$) following the methodology employed by Caffee et al. (1999) and Mukhopadhyay (2012). Because of the larger analytical uncertainty of ^{130}Xe-normalized ratios, we use ^{132}Xe-normalized ratios.

We assume the present-day mantle source values represent a mixture of four end-members: initial Xe, ^{238}U-produced Xe, ^{244}Pu-produced Xe, and subducted atmospheric Xe. The solution x to the system $Ax=b$ was found by a least-squares inversion with the additional constraints $\Sigma x_i=1$ and $0 \leq x_i \leq 1$. A is a matrix that defines the four end-members in terms of the four isotope ratios; x is a vector that defines the fraction of each of the four components in the present-day composition; and b is a vector with the mantle source compositions (free of post-eruptive air contamination). To determine the elements of b, the mantle source ^{129}Xe/^{132}Xe$_E$ was first determined from an Ar–Xe least-squares hyperbolic fit (Fig. S1). ^{130,131,134,136}Xe/^{132}Xe ratios were then linearly regressed against the ^{129}Xe/^{132}Xe ratio for the individual step-crushes. The linear regressions followed the same procedure as in Section 2.3 (see also Fig. 2). The slope and uncertainty in slope from the regressions were used to calculate the mantle ^{130,131,134,136}Xe/^{132}Xe$_E$ ratios along with their uncertainties for the given mantle ^{129}Xe/^{132}Xe$_E$ ratio. End-member and mantle source compositions (A and b, respectively) were normalized to the standard deviations in the mantle source isotope ratios to assign equal weight to each isotope ratio. To compute the uncertainties in the deconvolution, a Monte Carlo technique was utilized; the mantle source compositions were varied at random within their 1σ uncertainties and the least-squares fit recomputed using the new values. For all simulations it was verified that convergence to a minimum was achieved.

3. Results

3.1. Depleted MORB noble gases

Samples between the Ascension and Chain fracture zones have been previously classified as depleted MORBs on the basis of isotopic and incompatible element ratios (Schilling et al., 1994). We note that the depleted MORB samples span the range of extremely depleted MORBs (^{206}Pb/^{204}Pb=17.68; ^{87}Sr/^{86}Sr=0.7021) to MORBs showing an average degree of depletion (^{206}Pb/^{204}Pb=18.35; ^{87}Sr/^{86}Sr= 0.7026).

The ^{4}He/^{3}He ratios of the depleted MORBs vary between 80,800–86,700 with the more depleted Sr, Nd, and Pb isotopic composition associated with the lower ^{4}He/^{3}He ratios (Figs. 3 and S2a). ^{21}Ne/^{22}Ne$_E$ values for the depleted MORB samples range from 0.062 to 0.065 (Table 1; Figs. 2, 4 and S2b). For the depleted MORBs, the He and Ne isotopic compositions are negatively correlated (Fig. 5).

The highest measured ^{40}Ar/^{36}Ar ratio in the depleted samples is $30,400 \pm 300$. We note that sample RC2806 3D-2 has a lithophile isotopic composition very similar to average N-MORB source (^{206}Pb/^{204}Pb=18.35, ^{87}Sr/^{86}Sr=0.7026, ^{143}Nd/^{144}Nd=0.513126; cf. DMM: 18.275, 0.70263, 0.51313, Workman and Hart, 2005) and is also the only depleted sample for which the mixing hyperbolas in Ne–Ar–Xe space are well defined. Since the He and Ne isotopic composition of the depleted MORBs vary over a limited range, the Ar and Xe isotopic composition of the depleted samples may also show limited variations. However, given the sample's lithophile isotopic composition, and in the absence of substantial number of step-crushes for the other samples, we assume the extrapolated Ar and Xe isotopic composition for RC2806 3D-2 is broadly representative of the depleted group. The best fit hyperbola for this sample yields a mantle source ^{40}Ar/^{36}Ar$_E$ of $41,500 \pm 9000$ (Table 1; Fig. 6a). The uncertainty in ^{40}Ar/^{36}Ar$_E$ is related to a small number of data points with respect to the scatter in the data and suggests additional measurements on this sample in the future will be able to better constrain the hyperbolic fit. For a consistent comparison, we refit the step-crushing popping rock data (Moreira et al., 1998) using the same
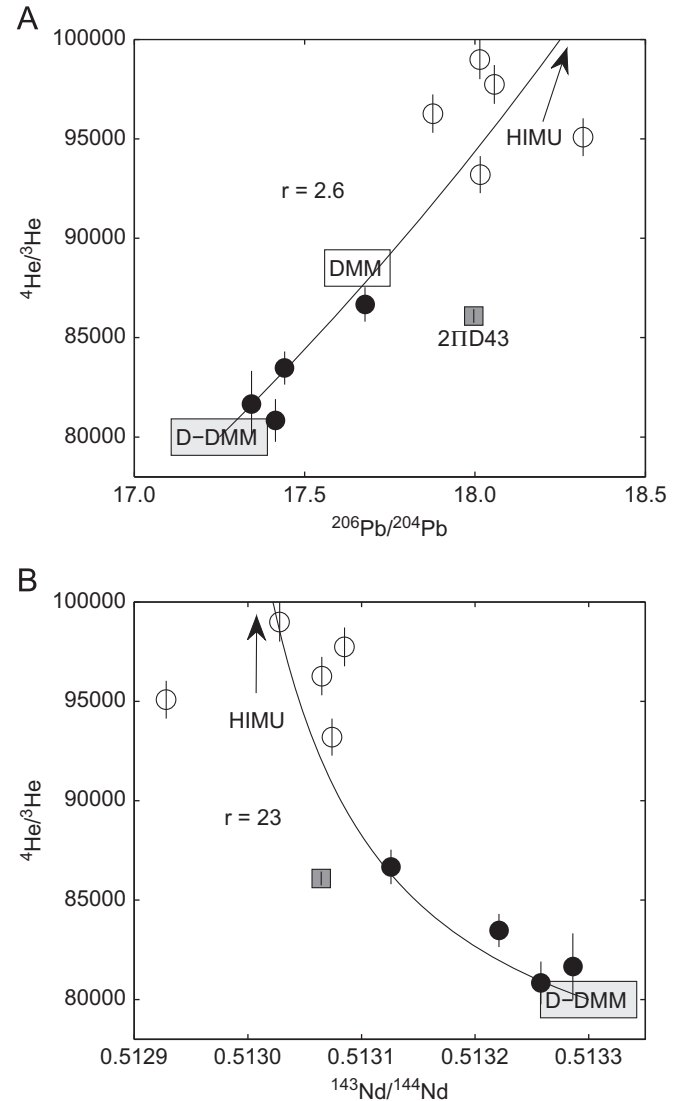

Fig. 3. Relationship between ^{4}He/^{3}He ratios and (a) ^{206}Pb/^{204}Pb and (b) ^{143}Nd/^{144}Nd. The solid symbols are the depleted MORBs and the open symbols are the enriched HIMU-type MORBs. He shows a coherent relationship with the other lithophile isotopes and indicates that more radiogenic He isotope ratios are associated with more radiogenic Pb and unradiogenic Nd, consistent with the presence of recycled material in the source of HIMU-type MORBs. The popping rock (2ΠD43) from the North Mid-Atlantic Ridge is indicated by the square. Popping rock data is from Moreira et al. (1998) and Dosso et al. (1991). He data for the samples EN061 2D and EN061 4D are from Graham et al. (1992b). The solid lines are illustrative two-component mixing hyperbolas between a depleted mantle (D-DMM) and a HIMU plume component. The ^{206}Pb/^{204}Pb ratios of D-DMM and HIMU are taken to be 17.5 and 23, and the ^{143}Nd/^{144}Nd ratios of D-DMM and HIMU are taken to be 0.51330 and 0.51295, respectively. The ^{4}He/^{3}He ratio of D-DMM is 80,000, similar to the low end of plume-free MORB (Graham, 2002), and the ^{4}He/^{3}He ratio of HIMU is 160,000, similar to the highest values measured at HIMU OIB (Graham et al., 1992a). The curvature of the hyperbola is controlled by the parameter r, defined as, e.g., $(^{3}$He/^{204}Pb$)_{D-DMM}/(^{3}$He/^{204}Pb$)_{HIMU}$.

technique (Section 2.3), which yielded a mantle source ^{40}Ar/^{36}Ar$_E$ of $25,200 \pm 600$ (Fig. 6a), consistent with the estimate of $27,000 \pm 4000$ from UV laser ablation of individual bubbles (Raquin et al., 2008).

The highest measured ^{129}Xe/^{130}Xe in the depleted sample group is 7.81 ± 0.06. Xe isotopes (^{129}Xe/^{130}Xe) correlate better with Ar isotopes than with Ne isotopes. Consequently, we obtained the best-fit hyperbola in Ar–Xe space for sample RC2806 3D-2 to constrain the mantle source ^{129}Xe/^{130}Xe$_E$ to 7.77 ± 0.06 at a ^{40}Ar/^{36}Ar of 41,500 (Table 1; Fig. 7a). Because of

Table 1
Mantle source compositions.

		$^{21}Ne/^{22}Ne$	$^{40}Ar/^{36}Ar$	$^{129}Xe/^{130}Xe$	$^{129}Xe/^{132}Xe$	$^{130}Xe/^{132}Xe$	$^{131}Xe/^{132}Xe$	$^{134}Xe/^{132}Xe$	$^{136}Xe/^{132}Xe$
Depleted MORB		0.0618	41,500	7.77	1.118	0.1449	0.7626	0.4306	0.3851
(present study)	1σ	0.0003	9000	0.06	0.008	0.0004	0.0017	0.0011	0.0012
Popping rock[a]		0.0598	27,000	7.5					
	1σ	0.0003	4000	0.06					
Bravo Dome[c]		0.0578	41,050	7.90					
	1σ	0.0003	2670	0.14					
Iceland[b]		0.0374	10,750	6.98					
	1σ	0.0001	3080	0.04					
HIMU-type MORB		0.0610	18,100	7.21	1.073	0.1488	0.7772	0.4118	0.3591
(present study)	1σ	0.0002	600	0.02	0.006	0.0003	0.0011	0.0007	0.0007

[a] Popping rock data is from Moreira et al. (1998) and Raquin and Moreira (2009); $^{129}Xe/^{130}Xe$ is based on a Ar–Xe hyperbolic fit using a mantle source $^{40}Ar/^{36}Ar$ ratio of 27,000.
[b] Iceland data is from Mukhopadhyay (2012).
[c] Bravo Dome data is from Holland and Ballentine (2006).

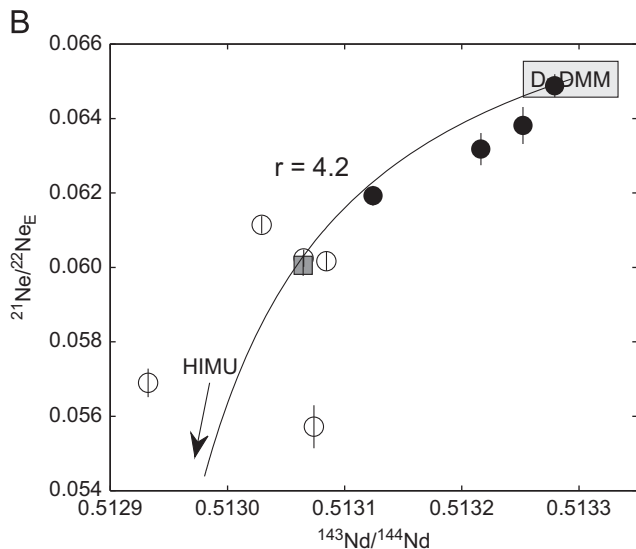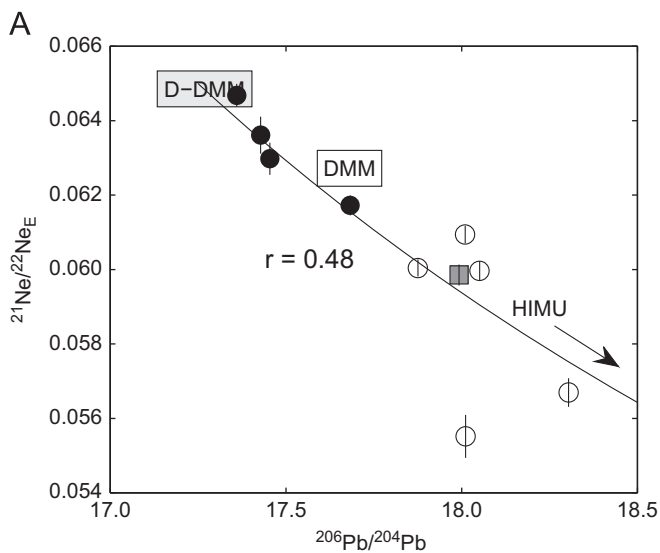**Fig. 4.** Relationship between $^{21}Ne/^{22}Ne_E$ ratios and (a) $^{206}Pb/^{204}Pb$ and (b) $^{143}Nd/^{144}Nd$. Symbols as in Fig. 3. The solid lines are illustrative two-component mixing hyperbolas for mixing between a depleted mantle (D-DMM) and the HIMU plume component. The Pb and Nd isotope ratios of the two components are as in Fig. 3. The $^{21}Ne/^{22}Ne$ ratio of D-DMM is 0.065 (this work) and the $^{21}Ne/^{22}Ne$ ratio of HIMU is 0.05 (Parai et al., 2009). The curvature of the hyperbola is controlled by the parameter r, defined as, e.g., $(^{22}Ne/^{204}Pb)_{D-DMM}/(^{22}Ne/^{204}Pb)_{HIMU}$.
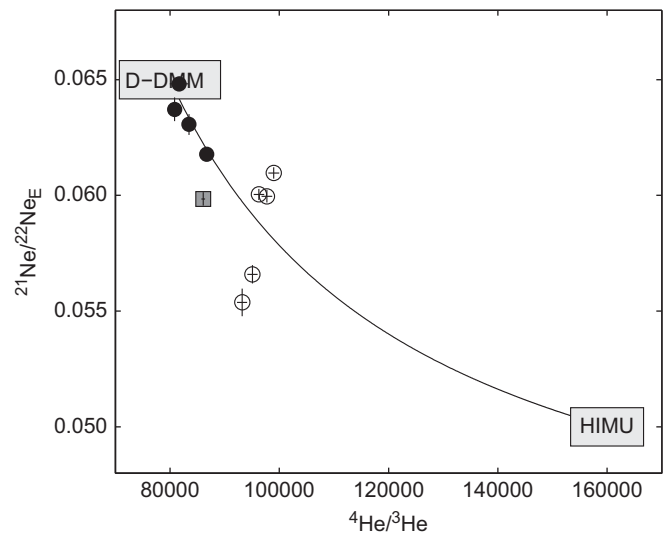

Fig. 5. Relationship between $^{4}He/^{3}He$ ratios and $^{21}Ne/^{22}Ne_E$ ratios. Symbols as in Fig. 3. Note that the sample with the most depleted Pb, Sr, and Nd isotopic composition has a lower $^{4}He/^{3}He$ ratio but higher nucleogenic $^{21}Ne/^{22}Ne_E$. Overall, there is a general tendency for increasing $^{4}He/^{3}He$ ratios to be associated with decreasing $^{21}Ne/^{22}Ne_E$ within the depleted MORB group. The HIMU-type MORBs are displaced to more radiogenic He and less nucleogenic Ne than the depleted MORBs. Overall, the He–Ne relationships of the MORBs can be explained by a mixture of depleted mantle (D-DMM) and HIMU, with the requirement that HIMU is composed of both recycled and less degassed mantle material, such as FOZO (Hart et al., 1992). The solid line is an illustrative mixing hyperbola using the end-member compositions as in Figs. 3 and 4. The curvature $r=(^{3}He/^{22}Ne)_{D-DMM}/(^{3}He/^{22}Ne)_{HIMU}=5.6$ is consistent with the hyperbolas in Figs. 3 and 4, e.g. $r_{He-Pb}/r_{Ne-Pb}=r_{He-Ne}$.

the curvature of the best-fit hyperbola, the mantle $^{129}Xe/^{130}Xe_E$ is not particularly sensitive to the uncertainty in $^{40}Ar/^{36}Ar_E$.

3.2. HIMU-type MORB noble gases

Samples north of the Romanche fracture zone are classified as enriched HIMU-type MORBs and span the range of $^{206}Pb/^{204}Pb$ from 18.75 to 19.64 and $^{87}Sr/^{86}Sr$ from 0.7026 to 0.7029. Although the Pb isotopic compositions in these samples do not reach the extreme HIMU compositions observed in OIBs, we refer to them as "HIMU-type" following the identification of a HIMU component in these basalts (Schilling et al., 1994) to distinguish them from the depleted MORBs south of the equator.

$^{4}He/^{3}He$ ratios of the HIMU-type MORBs are between 93,200 and 99,000—more radiogenic than the depleted MORBs
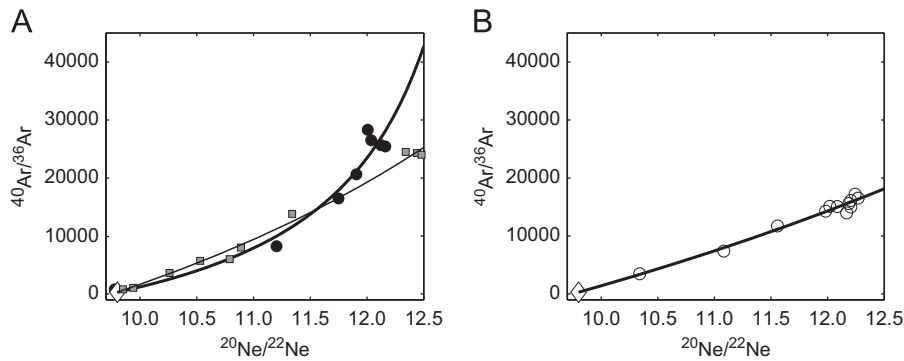
Fig. 6. (a) Ne–Ar hyperbola for the depleted MORB sample RC2806 3D-2 (thick solid line). Only crushes from the first aliquot are plotted as the crushes from the second aliquot define a poorly-constrained hyperbola with a different $(Ne/Ar)_{mantle}/(Ne/Ar)_{atm}$ ratio. The best-fit hyperbola to the step-crushes for popping rock (2ΠD43; Moreira et al., 1998) is shown for reference (thin line). Symbols as in Fig. 3 and the open diamond represents the atmospheric composition. (b) Ne–Ar hyperbolic fit for the HIMU-type MORB, RC2806 57D-1. Because of the curvature, the Ar isotopic composition of the mantle source corresponding to a mantle $^{20}Ne/^{22}Ne$ of 12.5 (Ballentine and Holland, 2008; Raquin et al., 2008) is well determined.
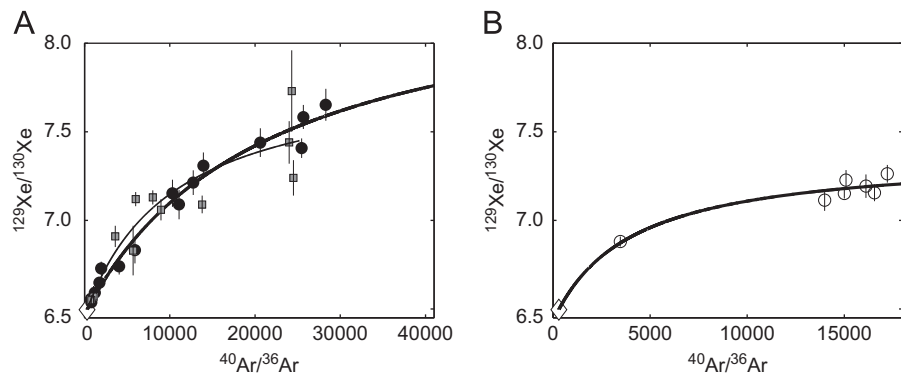

Fig. 7. (a) Ar–Xe mixing systematics for the depleted MORB RC2806 3D-2. Based on its lithophile isotopic composition this sample may be representative of average DMM in noble gas isotopic composition. The solid line is the best-fit hyperbola through the step-crushes. The best-fit hyperbola to the step-crushes for popping rock (2ΠD43) is shown for reference (thin line). The popping rock data is from Moreira et al. (1998). Symbols as in Fig. 3 and the open diamond represents the atmospheric composition. (b) Ar–Xe mixing systematics for the HIMU-type MORB, RC2806 57D-1. Note that the HIMU-type mantle source must have a lower $^{129}Xe/^{130}Xe$ ratio than DMM.

(Figs. 3 and S2a). $^{21}Ne/^{22}Ne_E$ values for the HIMU-type MORB samples are between 0.056 and 0.061, which is *less nucleogenic* than the depleted MORBs (Table 1; Figs. 2, 4, 5 and S2b). The highest measured $^{40}Ar/^{36}Ar$ ratio in the HIMU-type lavas is $17,800 \pm 178$, significantly lower than the highest measured values in the depleted sample group. Sample RC2806 57D-1 yields the best mixing hyperbola in Ne–Ar space, which constrains the source $^{40}Ar/^{36}Ar_E$ ratio to be $18,100 \pm 600$ (Table 1; Fig. 6b) and, like for the depleted MORB group, we assume this sample's Ar and Xe isotopic composition is broadly representative of the enriched HIMU-type MORBs. The highest measured $^{129}Xe/^{130}Xe$ in the depleted sample group is 7.26 ± 0.05. The Ar–Xe mixing array for the same sample (RC2806 57D-1) defines the mantle source $^{129}Xe/^{130}Xe_E$ of 7.21 ± 0.02 at a $^{40}Ar/^{36}Ar$ of 18,100 (Table 1; Fig. 7b). The curvature of the best-fit hyperbola indicates that $^{129}Xe/^{130}Xe_E$ is not particularly sensitive to the uncertainty in the mantle $^{40}Ar/^{36}Ar$.

3.3. A note on the mantle $^{20}Ne/^{22}Ne$ ratio

We recognize that the $^{20}Ne/^{22}Ne$ value of the whole mantle may not be 12.5, and the source of mantle plumes may be associated with $^{20}Ne/^{22}Ne$ of 12.9, or higher (Mukhopadhyay, 2012; Yokochi and Marty, 2004). We choose a MORB source value of 12.5 based on the mantle source composition of continental well gases (Ballentine and Holland, 2008; Holland and Ballentine, 2006) and the gas-rich popping rock (Raquin et al., 2008). Furthermore, our highest

measured value in both sample groups (12.36 in depleted samples; 12.43 in HIMU-type samples), and MORBs in general (Kunz, 1999; Moreira et al., 1998, 2011; Raquin and Moreira, 2009; Sarda et al., 1988) are close to 12.5. Correcting all the isotope ratios to a common $^{20}Ne/^{22}Ne$ allows for a consistent comparison between samples. Our primary results are not affected if a higher value is chosen. For example, if the mantle $^{20}Ne/^{22}Ne$ and $^{21}Ne/^{22}Ne$ varied as a mixture between the "MORB array" (12.5, 0.059; Sarda et al., 1988) and "Iceland array" (13.8, 0.0375; Mukhopadhyay, 2012) the least nucleogenic sample in our dataset would intersect this mixture at $^{20}Ne/^{22}Ne = 12.65$, causing a negligible shift in the extrapolated $^{40}Ar/^{36}Ar_E$ and $^{129}Xe/^{130}Xe_E$. If the mantle $^{20}Ne/^{22}Ne$ of the MORB source were higher than ~ 13, our results would actually be strengthened. Because of the curvature of the hyperbolas (Figs. 6 and 7), the depleted sample would extrapolate to higher $^{40}Ar/^{36}Ar$ and $^{129}Xe/^{130}Xe$ while the HIMU-type sample would be little affected, amplifying the compositional difference between them.

4. Discussion

4.1. A primitive Ne component in HIMU-type basalts

The $^4He/^3He$ ratios in the HIMU-type MORBs span the range of $\sim 80,000–100,000$, within the typical MORB range (Graham, 2002). The $^4He/^3He$ ratios of the HIMU-type lavas are, however, all more radiogenic than the depleted MORBs and are associated

with more radiogenic $^{206}Pb/^{204}Pb$ (Fig. 3). Since HIMU mantle plumes are characterized by radiogenic He and Pb isotopic ratios (Chauvel et al., 1992; Day and Hilton, 2011; Graham et al., 1992a; Hanyu et al., 1999; 2011; Hauri and Hart, 1993; Hilton et al., 2000; Parai et al., 2009), the He–Pb co-variation is consistent with the injection of a HIMU-type plume into the Equatorial Mid-Atlantic Ridge (Schilling et al., 1994).

The relationship between Ne and He isotopic compositions provides insight into the genesis of the HIMU plume sampled at the equatorial Mid-Atlantic Ridge. HIMU plumes are often assigned to recycled oceanic crust (Chauvel et al., 1992; Hauri and Hart, 1993; Hofmann, 1997). In addition to radiogenic $^{206}Pb/^{204}Pb$, such a component should have both radiogenic He and nucleogenic Ne isotopic ratios. This is because in highly degassed oceanic crust, nucleogenic ^{21}Ne will be produced from $^{18}O(\alpha,n)$ and $^{24}Mg(n,\alpha)$ reactions with the reacting alpha particles and neutrons ultimately sourced from U and Th decay. Thus, the less nucleogenic Ne in the HIMU-type lavas compared to the depleted MORBs cannot be generated solely through sampling of recycled material or mixing recycled material with DMM.

Our observation of less nucleogenic Ne and more radiogenic He have been observed in other HIMU localities, such as the Cameroon line of volcanoes (Barfod et al., 1999) and the Cook–Austral islands (Parai et al., 2009). The simplest explanation for the less nucleogenic signature is the involvement of a relatively undegassed mantle, such as FOZO. In this regard, Parai et al. (2009) attributed the association of more radiogenic He than MORBs with less nucleogenic Ne in the HIMU Cook–Austral islands to mixing between degassed recycled crust and FOZO (also see Day and Hilton, 2011). Based on the lithophile isotopes, Schilling et al. (1994) suggested that the plume-influenced MORBs north of the equator reflect mixing between a depleted mantle, recycled crust (HIMU) and FOZO. Our present study is consistent with the suggestion of a HIMU component in the north equatorial Atlantic MORBs (Schilling et al., 1994) and provides further evidence that HIMU is a hybrid of at least two different materials—a degassed recycled component and a relatively undegassed mantle.

4.2. A negative correlation between He and Ne in depleted MORBs

Our new observations from the equatorial Atlantic indicate that within the depleted group there appears to be an overall trend of *more* nucleogenic $^{21}Ne/^{22}Ne_E$ associated with *less* radiogenic He and more depleted Sr, Nd and Pb isotopic compositions (Figs. 3–5). This observation places constraints on the $^{4}He/^{3}He$ and $^{21}Ne/^{22}Ne_E$ variability in MORBs, and the relationship between the most depleted MORBs (D-DMM; Workman and Hart, 2005) and N-MORBs (DMM).

Helium and neon isotopic variations in the MORB source are often interpreted in terms of a flux of ^{3}He and ^{22}Ne from the OIB source into the MORB source followed by mixing with in situ radiogenic ^{4}He and nucleogenic ^{21}Ne (e.g. Allegre et al., 1987; Porcelli and Wasserburg, 1995; Tolstikhin and Hofmann, 2005). However, differences in $^{20}Ne/^{22}Ne$ and $^{3}He/^{22}Ne$ ratios between MORBs and OIBs suggests that not all the primordial He and Ne in the MORB mantle can be derived from the OIB mantle source (Honda and McDougall, 1998; Mukhopadhyay, 2012; Yokochi and Marty, 2004). Assuming ^{3}He is indigenous to the MORB source, variations in MORB $^{4}He/^{3}He$ ratios may be explained in the framework of a marble cake assemblage comprising pyroxenite veins in a depleted peridotite matrix (e.g. Graham et al., 2001; Hamelin et al., 2011). The $^{4}He/^{3}He$ ratio of the most depleted MORB in our dataset lies at the lower limit of the MORB range from 74,000 to 120,000 for regions removed from obvious influences of mantle plumes (Georgen et al., 2003; Graham,

2002; Graham et al., 1992b, 2001). The addition of pyroxenites (recycled crust) with radiogenic ^{4}He to this depleted peridotitic matrix could then produce the range of $^{4}He/^{3}He$ ratios and lithophile isotopes in non-plume influenced MORBs (Figs. 3 and S2a). Within the marble cake framework, recycled oceanic crust should be associated with nucleogenic $^{21}Ne/^{22}Ne$ ratios in addition to radiogenic $^{4}He/^{3}He$ ratios. So as $^{4}He/^{3}He$ ratios become more radiogenic in MORBs through sampling a greater proportion of pyroxenites, $^{21}Ne/^{22}Ne$ ratios should become more nucleogenic, opposite to the observed relation between He and Ne (Fig. 5). Hence, the observed isotopic relations (Figs. 3–5) cannot be generated by mixing depleted peridotites with pyroxenites that have radiogenic He and nucleogenic Ne.

Instead, we hypothesize that the observed He–Ne relationship requires the equatorial Atlantic N-MORBs to be produced by the addition of a small proportion of a HIMU plume component to a very depleted MORB source (D-DMM; e.g. Fig. 5). We note that based on lithophile isotopes Schilling et al. (1994) suggested that the depleted section of the Mid-Atlantic Ridge between the Ascension and Romanche fracture zones resulted from mixing between an extremely depleted MORB source and an enriched HIMU component. Our results are consistent with this interpretation with the additional requirement that HIMU is itself a mixture of recycled and primitive components (Section 4.1). While a marble cake mantle remains a viable way of interpreting the geochemical observations in depleted MORBs, based on our new He–Ne observations, it appears to be richer in flavor than a simple mixture of recycled pyroxenites and depleted peridotites.

4.3. Argon isotopic composition of DMM and the HIMU-type MORB source

The depleted MORB sample RC2806 3D-2 has a mantle source $^{40}Ar/^{36}Ar_E$ ratio of $41,500 \pm 9000$ (Fig. 6a). This is similar to the $^{40}Ar/^{36}Ar$ ratio of $41,050 \pm 2670$ for the Bravo Dome well gas and the maximum measured $^{40}Ar/^{36}Ar$ in MORBs of $42,400 \pm 9700$ (Marty and Humbert, 1997). In contrast, we compute the popping rock mantle source $^{40}Ar/^{36}Ar_E$ to be $25,200 \pm 600$ from the published step-crushing data (Fig. 6a) (Moreira et al., 1998), similar to the value of 25,000 reported in that work and $27,000 \pm 4000$ obtained by UV laser ablation of individual bubbles (Raquin et al., 2008). We note that a laser ablation study by Burnard et al. (1997) yielded a $^{40}Ar/^{36}Ar$ ratio of $40,000 \pm 4000$ in an individual bubble in the popping rock sample, higher than the values reported by Raquin et al. (2008) and those of Moreira et al. (1998). While the mantle source composition of popping rock is debatable (see Raquin et al., 2008 for further discussion), DMM has a $^{40}Ar/^{36}Ar$ ratio of at least 41,000.

The HIMU-type MORB sample RC2806 57D-1 has a mantle source $^{40}Ar/^{36}Ar_E$ ratio of $18,100 \pm 600$, unequivocally lower than both DMM and the popping rock mantle source (Fig. 6b). The result demonstrates that large variations (factor of 2) in the MORB mantle source $^{40}Ar/^{36}Ar$ ratio exist even when variations in He and Ne isotopic compositions are more muted. The low $^{40}Ar/^{36}Ar_E$ ratio in the HIMU-type MORBs likely results from the injection of a HIMU mantle plume with low $^{40}Ar/^{36}Ar$ into the Mid-Atlantic Ridge. Plumes feeding OIB are often characterized by low $^{40}Ar/^{36}Ar$ (Honda et al., 1993; Mukhopadhyay, 2012; Raquin and Moreira, 2009; Trieloff et al., 2000, 2002; Valbracht et al., 1997). The low $^{40}Ar/^{36}Ar$ in plumes and the HIMU-type MORBs of the north equatorial Atlantic could be due to sampling of a less degassed reservoir with low $K/^{36}Ar$ ratio, an explanation that would be consistent with Ne isotopic evidence for a less degassed component in the HIMU plume. Alternatively, the low $^{40}Ar/^{36}Ar$ ratio could be a result of recirculation of atmospheric Ar associated with recycled crust to the mantle source of plumes

(Holland and Ballentine, 2006). We discuss these two separate hypotheses while discussing Xe isotopes in the next section.

4.4. Xenon isotopic differences between DMM, HIMU-type MORB and Iceland plume sources

The depleted MORB sample RC2806 3D-2 has a mantle source $^{129}Xe/^{130}Xe_E$ ratio of 7.77 ± 0.06 (Fig. 7a). This ratio overlaps with the $^{129}Xe/^{130}Xe$ ratio of 7.9 ± 0.14 for the mantle source of the Bravo Dome well gas (Holland and Ballentine, 2006). On the other hand, the HIMU-type MORB sample RC2806 57D-1 has a mantle source $^{129}Xe/^{130}Xe_E$ of 7.21 ± 0.05, significantly lower than the depleted MORB source (Fig. 7b). Like the less nucleogenic $^{21}Ne/^{22}Ne_E$ ratio and less radiogenic $^{40}Ar/^{36}Ar_E$ ratio, the lower $^{129}Xe/^{130}Xe_E$ in the HIMU-type MORBs could reflect sampling of a less degassed reservoir with a lower $I/^{130}Xe$ ratio than the DMM source. ^{129}I, which produces ^{129}Xe, became extinct at 4.45 Ga and therefore differences in the degree of degassing between DMM and the less degassed reservoir would have to have been initiated prior to 4.45 Ga and the reservoirs could not have subsequently been homogenized. Alternatively, the lower $^{129}Xe/^{130}Xe_E$ in the HIMU-type MORBs could reflect preferential recycling of atmospheric Xe into the HIMU plume source. These two hypotheses can be addressed by considering the $^{129}Xe/^{136}Xe$ ratio, which reflects the time-integrated $^{129}I/(^{244}Pu+^{238}U)$ ratio (Fig. 8).

Given the uncertainties in Xe isotopic ratios, we cannot yet identify possible Xe isotopic differences within the depleted or HIMU-type groups. As a result, in Fig. 8, we combine the step-crushes for each sample group to investigate whether differences in Xe isotopic composition exist between the depleted and HIMU-type groups and whether the depleted MORBs are isotopically distinct from the Iceland plume. Fig. 8a shows our data in $^{129}Xe/^{130}Xe$ vs. $^{136}Xe/^{130}Xe$ space. In this space, the Xe–Xe slopes for the depleted and HIMU groups are statistically distinct from each other and from the slope calculated for all the data taken together.

The distinct $^{129}Xe/^{136}Xe$ ratios for the two MORB groups can be clearly seen in $^{129}Xe/^{136}Xe$ vs. $^{130}Xe/^{136}Xe$ space when the error-weighted average compositions of the crushing steps are plotted (Fig. 8b). The data are not corrected for post-eruptive contamination, so the true mantle source (extrapolated) values lie further along the particular mixing line with air. But extrapolation is unnecessary to demonstrate the simple conclusion that the

HIMU-type MORBs have a $^{129}Xe/^{136}Xe$ ratio in excess of air while the depleted MORBs have a ratio lower than air. The data in Fig. 8, therefore, clearly demonstrate that the depleted MORBs and the HIMU-type MORBs have distinct $^{129}Xe/^{136}Xe$ ratios. Furthermore, a clear distinction is observed between the Iceland plume composition (Mukhopadhyay, 2012) and the depleted MORBs, with the HIMU-type MORBs intermediate between the two.

In both of the Xe–Xe isotopic spaces (Fig. 8a and b), recycling of atmospheric Xe would shift the composition of a reservoir linearly towards air. Thus, neither the small difference in slope (Fig. 8a) nor the measured difference in the $^{129}Xe/^{136}Xe$ ratio (Fig. 8b) between the depleted and HIMU-type MORBs can be produced solely through recycling of atmospheric Xe. We conclude that $^{129}I/(^{244}Pu+^{238}U)$ ratios are different between the two groups of MORBs, reflecting different degrees of mantle outgassing. The lower $^{129}Xe/^{136}Xe$ ratio of DMM is consistent with a more degassed source than the mantle source of HIMU-type MORBs (Fig. 8). This is because a more degassed source will have lower concentrations of primordial Xe isotopes (^{130}Xe), and lower concentrations of ^{129}Xe from decay of extinct ^{129}I and ^{136}Xe from fission of extinct ^{244}Pu. Adding ^{136}Xe from ^{238}U fission or ^{244}Pu fission while ^{244}Pu is still alive to such a degassed source will lead to a decrease in $^{129}Xe/^{136}Xe$ ratio. The higher $^{129}Xe/^{136}Xe$ ratio of the HIMU-type MORBs likely reflects mixing between a less degassed source, such as the reservoir supplying primordial noble gases to the Iceland plume (Mukhopadhyay, 2012), and more degassed sources, such as recycled crust and DMM. In this regard, the $^{129}Xe/^{136}Xe$ evidence suggests that the lower $^{40}Ar/^{36}Ar_E$ ratio in the HIMU-type MORBs also cannot originate solely from recycling of atmospheric Ar; sampling of a less degassed mantle reservoir with low $^{40}Ar/^{36}Ar$ ratio is required.

4.5. Pu–U–I derived Xe in the depleted and the HIMU-type MORB mantle source

The proportion of Pu- to U-derived Xe provides powerful independent constraints on the degree of outgassing of a mantle source that augments arguments from the other noble gas isotope ratios. Because fission Xe yields from Pu are significantly larger than from U, a reservoir that has remained completely closed over Earth's history will have $^{136}Xe^{*}_{Pu}/^{136}Xe^{*}_{U}$ of ~ 27, where '*' refers to fissiogenic Xe. Because ^{244}Pu became extinct at ~ 4 Ga, reservoirs open to substantial volatile loss over the past 4 billion years
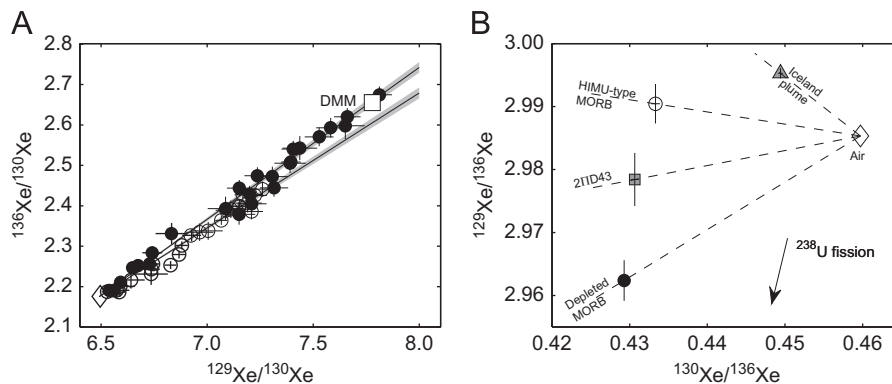

Fig. 8. (a) $^{129}Xe/^{130}Xe$ vs. $^{136}Xe/^{130}Xe$ ratios of step-crushes for depleted and HIMU-type MORB. Symbols as in Fig. 3. The solid lines represent the x–y error weighted best fit line and the gray bands denote the 1σ error envelopes. The methodology for the least squares regression was outlined in Section 2.3 and in Fig. 2. The slope of the line is a function of the time integrated $(^{244}Pu+^{238}U)/^{129}I$ ratio. The slopes are 0.375 ± 0.009 and 0.334 ± 0.009 for depleted and HIMU-type MORBs, respectively. The slope with all data taken together is 0.358 ± 0.006, which does not overlap the slope of either group. The difference in slopes demonstrates a difference in the time integrated $(^{244}Pu+^{238}U)/^{129}I$ ratio within MORBs. (b) $^{130}Xe/^{136}Xe$ vs. $^{129}Xe/^{136}Xe$ isotope plot showing the weighted average composition of DICE 10 (Iceland; Mukhopadhyay, 2012), depleted MORB and HIMU-type MORB step-crushes. Symbols as in Fig. 3. The air-Iceland mixing line is distinct from the air-depleted MORB mixing line. Consequently, the plume Xe signal cannot be related to MORBs solely through addition of subducted atmospheric Xe or through addition of ^{238}U-produced fission ^{136}Xe. Sampling of a reservoir that is less degassed than DMM is required to explain the Xe isotopic composition of the HIMU-type MORBs and the Iceland plume.

Table 2
Xenon components in the depleted MORB and HIMU-type MORB mantle sources.

Starting mantle composition	Sample	Fraction ^{132}Xe from recycled air	Fraction ^{132}Xe from SW[a]/AVCC[b]	Fraction ^{132}Xe from ^{238}U[c]	Fraction ^{132}Xe from ^{244}Pu[d]	Fraction ^{136}Xe from ^{244}Pu	^{129}Xe*/^{136}Xe*$_{Pu}$ [e]
Solar wind	Depleted MORBs	0.896 ± 0.054	0.058 ± 0.049	0.027 ± 0.004	0.019 ± 0.008	$0.29^{+0.14}_{-0.12}$	$8.9^{+6.5}_{-3.1}$
	HIMU-type MORBs	0.778 ± 0.041	0.188 ± 0.038	0.013 ± 0.003	0.022 ± 0.006	0.52 ± 0.13	$4.6^{+1.9}_{-1.0}$
AVCC	Depleted MORBs	0.910 ± 0.052	$0.046^{+0.049}_{-0.046}$	0.028 ± 0.005	0.017 ± 0.008	$0.25^{+0.17}_{-0.10}$	$10.7^{+7.4}_{-4.6}$
	HIMU-type MORBs	0.767 ± 0.047	0.201 ± 0.044	0.009 ± 0.004	0.023 ± 0.007	0.63 ± 0.18	$4.1^{+1.9}_{-1.0}$

[a] Pepin et al. (1995) and Wieler and Baur (1994).
[b] Pepin (1991, 2000).
[c] Porcelli et al. (2002) and references therein.
[d] Hudson et al. (1989).
[e] ^{129}Xe*/^{136}Xe*$_{Pu}$ is the ratio of radiogenic ^{129}Xe from decay of ^{129}I to fissiogenic ^{136}Xe derived from ^{244}Pu fission. The distributions of ^{129}Xe*/^{136}Xe*$_{Pu}$ are skewed and hence, the median and the 67% confidence intervals are presented. We use the following method to determine ^{129}Xe*/^{136}Xe*$_{Pu}$: once the fractions of initial ^{132}Xe and ^{132}Xe from recycled air are calculated, the ^{129}Xe/^{132}Xe ratio of the mantle source (Fig. S1) defines the fraction of ^{129}Xe produced from decay of ^{129}I (^{129}Xe*). Combining this with the Pu-derived fission ^{136}Xe yields the ^{129}Xe*/^{136}Xe*$_{Pu}$ ratio.

will have a large proportion of fission Xe derived from ^{238}U; i.e., ^{136}Xe*$_{Pu}$/^{136}Xe*$_U$ in degassed reservoirs will be $\ll 27$ (Kunz et al., 1998; Ozima et al., 1985; Tolstikhin and O'Nions, 1996; Yokochi and Marty, 2005).

In the present day mantle, ^{131,132,134,136}Xe isotopes reflect a mixture of the initial mantle Xe, Pu- and U-produced fission Xe, and subducted atmospheric Xe, if any. For the initial mantle composition we investigated solar and chondritic Xe (AVCC) (Caffee et al., 1999; Holland and Ballentine, 2006; Holland et al., 2009; Pujol et al., 2011). The deconvolution of the four Xe components was performed with the mantle source ratios listed in Table 1 and the methodology discussed in Section 2.4. Here we will note four major implications of the fission deconvolution: (a) recycling of atmospheric Xe to the mantle, (b) the ratio of Pu- to U-derived Xe in the depleted MORB source, (c) the ratio of Pu- to U-derived Xe in the HIMU-type MORB source, and (d) I/Pu ratios in the depleted and HIMU-type MORB sources.

For a mantle starting composition of either solar Xe or chondritic Xe, substantial injection of atmospheric Xe back into the mantle is required. We find that on order 80–90% of the ^{132}Xe in the mantle source is derived from recycled atmospheric Xe (Table 2). The proportion of recycled Xe in the HIMU-type MORBs, however, does not appear to be larger than in the depleted MORBs (Table 2). Thus, we suggest that the lower ^{129}Xe/^{130}Xe ratios in the enriched HIMU-type MORBs do not result from preferential recycling of atmospheric Xe into the plume source. Rather the HIMU-type MORBs must sample a reservoir with a lower ^{129}I/^{130}Xe than the depleted MORBs.

The requirement that a significant fraction of the fissiogenic Xe isotopes in the mantle is recycled from the atmosphere (Table 2) is consistent with previous work that suggests Xe can be recycled back into the mantle (Holland and Ballentine, 2006; Kendrick et al., 2011; Sumino et al., 2010). The recycling of atmospheric Xe could have happened all through Earth's history associated with plate subduction (Holland and Ballentine, 2006), or very early on in Earth's history (Moreira and Raquin, 2007). However, since the ^{129}Xe/^{130}Xe ratio can only evolve during the first 100 Myr of solar system history, the distinct atmospheric and mantle compositions require that recycling efficiency of atmospheric Xe must be relatively low so as not to homogenize the mantle and atmospheric compositions over 4.45 Ga. In this regard, since at most 80–90% of the Xe in the mantle is recycled (Table 2), the mantle ^{129}Xe/^{130}Xe ratio can still be distinctly different from the atmospheric ratio.

Depending on whether the initial mantle Xe composition is solar or chondritic, the fraction of ^{136}Xe derived from Pu fission in the depleted MORB source is $0.25^{+0.17}_{-0.10}$ or $0.29^{+0.14}_{-0.12}$, respectively (Table 2). The corresponding ^{136}Xe*$_{Pu}$/^{136}Xe*$_U$ is 0.33 ± 0.12 or 0.41 ± 0.1. The ^{136}Xe*$_{Pu}$/^{136}Xe*$_U$ ratios are ~1% of the closed system value of 27 and suggest that the depleted MORB source has lost 99% of its Pu-produced Xe as a result of mantle outgassing from a combination of giant impacts and mantle convection.

In the HIMU-type MORB source, the fraction of ^{136}Xe derived from Pu fission is 0.52 ± 0.13 (solar) or 0.63 ± 0.18 (chondritic) (Table 2). Although the uncertainties are large, the result suggests that the HIMU-type MORBs may have a higher proportion of Pu- to U-derived fission Xe than the depleted MORBs but lower than the Iceland plume (Table 2; see also Fig. S3). The high proportion of Pu-derived Xe in the HIMU-type MORBs compared to the depleted MORBs is inconsistent with the HIMU component being comprised only of recycled crust or a mixture of recycled crust and DMM. This is because recycled crust should be highly degassed and will have fission Xe produced only from ^{238}U fission during its residence in the mantle. Pu-produced Xe could be present in recycled crust only if the crust were produced and subducted back into mantle prior to 4 Ga when ^{244}Pu was still alive. However, Re–Os and Pb isotopic systematics indicate an age of 1–2 Ga for the HIMU mantle (Chauvel et al., 1992; Hauri and Hart, 1993). Therefore, the relatively high proportion of Pu- to U-derived fission Xe in the HIMU-type mantle provides further evidence that HIMU is a hybrid of a recycled and a less degassed mantle component and requires the Xe contribution from the less degassed mantle component to dominate over the ^{238}U-produced fission Xe in the recycled crust. Such a conclusion is consistent with the HIMU-type MORBs having a ^{129}Xe/^{136}Xe ratio that is intermediate between Iceland and the depleted MORBs.

The combined I–Pu–Xe system has been used to constrain the closure time for volatile loss of a mantle reservoir through the ^{129}Xe*/^{136}Xe*$_{Pu}$ ratio, where ^{129}*Xe is the decay product of ^{129}I decay and ^{136}Xe*$_{Pu}$ is ^{136}Xe produced from ^{244}Pu fission (Allegre et al., 1987; Azbel and Tolstikhin, 1993; Kunz et al., 1998; Ozima et al., 1985; Pepin and Porcelli, 2006; Yokochi and Marty, 2005). ^{129}I has a shorter half-life than ^{244}Pu and as a result, higher ^{129}Xe*/^{136}Xe*$_{Pu}$ ratios are indicative of earlier closure to volatile loss. We find that for the depleted MORB source, the ^{129}Xe*/^{136}Xe*$_{Pu}$ ratio is $10.7^{+7.4}_{-4.6}$ or $8.9^{+6.5}_{-3.1}$ depending on an initial mantle composition of solar or chondritic Xe; the ^{129}Xe*/^{136}Xe*$_{Pu}$ for the HIMU-type MORB source is $4.1^{+1.9}_{-1.0}$ or $4.6^{+1.9}_{-1.0}$ (Table 2).

Interpreting these values as closure ages for a mantle with an initially homogenous I/Pu ratio, the higher $^{129}Xe^*/^{136}Xe^*_{Pu}$ ratio in the depleted MORB source would imply that the shallow upper mantle became closed to volatile loss prior to the deep mantle reservoir supplying noble gases to the HIMU plume. Such a conclusion appears paradoxical. Rather, a simpler explanation is that the lower $^{129}Xe^*/^{136}Xe^*_{Pu}$ in the HIMU-type MORB source reflects a lower initial I/Pu ratio for the plume source compared to the MORB source. This is consistent with the conclusions inferred from the Xe data in the Iceland plume (Mukhopadhyay, 2012) and suggests that the initial phase of Earth's accretion was volatile poor compared to the later stages of accretion because Pu is a refractory element while I is a volatile element.

Differences in I/Pu ratios and I/Xe ratios in the mantle are relicts of accretion and early Earth processes. The preservation of these differences in the present day mantle reflects the relatively low recycling efficiency of the noble gases with respect to the lithophile and siderophile elements. Importantly, since ^{129}I became extinct 100 Myr after the start of the solar system, the differences in $^{129}Xe/^{130}Xe_E$ ratios (Fig. 7) between the reservoir supplying Xe to the Iceland and HIMU plumes and DMM must have been established by 4.45 Ga. If the two reservoirs were completely homogenized after 4.45 Ga, the different Xe isotopic compositions in the present day mantle could not have been maintained.

5. Conclusions

We present new heavy noble gas data in MORBs from the equatorial Mid-Atlantic Ridge. Based on our observations we conclude:

1. He–Ne are tightly coupled to variations in the lithophile isotopes. The depleted end of the MORB array (D-DMM) is less radiogenic in He but more nucleogenic in Ne than N-MORBs (DMM). We conclude that N-MORBs in the equatorial Atlantic are produced by mixing a small proportion of a HIMU plume component to a very depleted MORB matrix.
2. Despite having more radiogenic Pb and He isotopic compositions, the HIMU-type MORB mantle source is less nucleogenic in $^{21}Ne/^{22}Ne$ and less radiogenic $^{40}Ar/^{36}Ar$ and $^{129}Xe/^{130}Xe$ ratios than DMM. $^{129}Xe/^{136}Xe$ ratios preclude air or seawater subduction as the sole cause of the lower $^{129}Xe/^{130}Xe_E$ in the HIMU-type MORB source compared to the depleted MORB source; a less degassed component is required in the HIMU source. Consequently, the lower $^{21}Ne/^{22}Ne_E$, $^{40}Ar/^{36}Ar_E$ and $^{129}Xe/^{130}Xe_E$ are also interpreted as evidence for a less degassed mantle reservoir contributing to the HIMU plume. We emphasize that our results do not imply that air or seawater subduction do not occur; rather by itself it cannot account for the differences between the two groups of MORBs.
3. The ratio of Pu- to U-derived fission ^{136}Xe in the depleted MORB source is ~0.4, suggesting it has lost 99% of its Pu-derived Xe, and thus at least 99% of its original primordial volatile inventory. The HIMU-type MORBs have a higher ratio of Pu- to U-derived fission Xe than the depleted MORB group, consistent with the sampling of a less degassed mantle reservoir in the HIMU plume.
4. Differences in $^{129}Xe^*/^{136}Xe^*_{Pu}$ suggest a lower I/Pu ratio for the relatively undegassed mantle reservoir compared to the depleted MORB source and thus supports heterogeneous volatile accretion with early accretion being drier than later accreting material. Overall the Xe isotopic compositions require the preservation of early (pre-4.45 Ga) formed heterogeneities in the present day mantle.

Appendix A. Supplementary materials

Supplementary data associated with this article can be found in the online version at http://dx.doi.org/10.1016/j.epsl.2012.08.025.

References

Agranier, A., Blichert-Toft, J., Graham, D., Debaille, V., Schiano, P., Albarede, F., 2005. The spectra of isotopic heterogeneities along the mid-Atlantic Ridge. Earth Planet. Sci. Lett. 238, 96–109.

Allegre, C.J., Hofmann, A., O'Nions, K., 1996. The Argon constraints on mantle structure. Geophys. Res. Lett. 23, 3555–3557.

Allegre, C.J., Staudacher, T., Sarda, P., Kurz, M., 1983. Constraints on the evolution of Earth's mantle from rare gas systematics. Nature 303, 762–766.

Allegre, C.J., Staudacher, T., Sarda, P., 1987. Rare gas systematics: formation of the atmosphere, evolution and structure of the Earth's mantle. Earth Planet. Sci. Lett. 81, 127–150.

Azbel, I.Y., Tolstikhin, I.N., 1993. Accretion and early degassing of the Earth: constraints from Pu-U-I-Xe isotopic systematics. Meteoritics 28, 609–621.

Ballentine, C.J., Holland, G., 2008. What CO$_2$ well gases tell us about the origin of noble gases in the mantle and their relationship to the atmosphere. Philos. Trans. R. Soc. A: Math., Phys. Eng. Sci. 366, 4183–4203.

Barfod, D.N., Ballentine, C.J., Halliday, A.N., Fitton, J.G., 1999. Noble gases in the Cameroon line and the He, Ne, and Ar isotopic compositions of high μ (HIMU) mantle. J. Geophys. Res. 104, 29509–29527.

Burnard, P., Graham, D., Turner, G., 1997. Vesicle-specific noble gas analyses of "popping rock": implications for primordial noble gases in Earth. Science 276, 568–571.

Burnard, P.G., 1999. Origin of argon–lead isotopic correlation in basalts. Science 286, 871a.

Caffee, M.W., Hudson, G.B., Velsko, C., Huss, G.R., Alexander Jr., E.C., Chivas, A.R., 1999. Primordial noble gases from Earth's mantle: identification of a primitive volatile component. Science 285, 2115–2118.

Chauvel, C., Hofmann, A.W., Vidal, P., 1992. HIMU-EM: the French Polynesian connection. Earth Planet. Sci. Lett. 110, 99–119.

Coltice, N., Moreira, M., Hernlund, J., Labrosse, S., 2011. Crystallization of a basal magma ocean recorded by helium and neon. Earth Planet. Sci. Lett. 308, 193–199.

Day, J.M.D., Hilton, D.R., 2011. Origin of $^3He/^4He$ ratios in HIMU-type basalts constrained from Canary Island lavas. Earth Planet. Sci. Lett. 305, 226–234.

Dosso, L., Bougault, H., Joron, J.-L., 1993. Geochemical morphology of the North Mid-Atlantic Ridge, 10–24°N: trace element-isotope complementarity. Earth Planet. Sci. Lett. 120, 443–462.

Dosso, L., Hanan, B.B., Bougault, H., Schilling, J.-G., Joron, J.-L., 1991. Sr–Nd–Pb geochemical morphology between 10° and 17°N on the Mid-Atlantic Ridge: a new MORB isotope signature. Earth Planet. Sci. Lett. 106, 29–43.

Gayer, E., Mukhopadhyay, S., Meade, B.J., 2008. Spatial variability of erosion rates inferred from the frequency distribution of cosmogenic ^3He in olivines from Hawaiian river sediments. Earth Planet. Sci. Lett. 266, 303–315.

Georgen, J.E., Kurz, M.D., Dick, H.J.B., Lin, J., 2003. Low $^3He/^4He$ ratios in basalt glasses from the western Southwest Indian Ridge (10°–24°E). Earth Planet. Sci. Lett. 206, 509–528.

Gonnermann, H.M., Mukhopadhyay, S., 2009. Preserving noble gases in a convecting mantle. Nature 459, 560–563.

Graham, D.W., Humphris, S.E., Jenkins, W.J., Kurz, M.D., 1992a. Helium isotope geochemistry of some volcanic rocks from Saint Helena. Earth Planet. Sci. Lett. 110, 121–131.

Graham, D.W., Jenkins, W.J., Schilling, J.-G., Thompson, G., Kurz, M.D., Humphris, S.E., 1992b. Helium isotope geochemistry of Mid-Ocean Ridge basalts from the South Atlantic. Earth Planet. Sci. Lett. 110, 133–147.

Graham, D.W., Lupton, J.E., Spera, F.J., Christie, D.M., 2001. Upper-mantle dynamics revealed by helium isotope variations along the southeast Indian ridge. Nature 409, 701–703.

Graham, D.W., 2002. Noble gas isotope geochemistry of mid-ocean ridge and ocean island basalts: characterization of mantle source reservoirs. Rev. Mineral. Geochem. 47, 247.

Hamelin, C., Dosso, L., Hanan, B.B., Moreira, M., Kositsky, A.P., Thomas, M.Y., 2011. Geochemical portray of the Pacific Ridge: new isotopic data and statistical techniques. Earth Planet. Sci. Lett. 302, 154–162.

Hannigan, R.E., Basu, A.R., Teichmann, F., 2001. Mantle reservoir geochemistry from statistical analysis of ICP-MS trace element data of equatorial mid-Atlantic MORB glasses. Chem. Geol. 175, 397–428.

Hanyu, T., Kaneoka, I., Nagao, K., 1999. Noble gas study of HIMU and EM ocean island basalts in the Polynesian region. Geochim. Cosmochim. Acta 63, 1181–1201.

Hanyu, T., Tatsumi, Y., Kimura, J.-I., 2011. Constraints on the origin of the HIMU reservoir from He–Ne–Ar isotope systematics. Earth Planet. Sci. Lett. 307, 377–386.

Hart, S.R., Hauri, E.H., Oschmann, L.A., Whitehead, J.A., 1992. Mantle plumes and entrainment—isotopic evidence. Science 256, 517–520.

Hauri, E.H., Hart, S.R., 1993. Re–Os isotope systematics of HIMU and EMII oceanic island basalts from the South-Pacific Ocean. Earth Planet. Sci. Lett. 114, 353–371.

Hilton, D.R., Macpherson, C.G., Elliott, T.R., 2000. Helium isotope ratios in mafic phenocrysts and geothermal fluids from La Palma, the Canary Islands (Spain): implications for HIMU mantle sources. Geochim. Cosmochim. Acta 64, 2119–2132.

Hofmann, A.W., 1997. Mantle geochemistry: the message from oceanic volcanism. Nature 385, 219–229.

Holland, G., Ballentine, C.J., 2006. Seawater subduction controls the heavy noble gas composition of the mantle. Nature 441, 186–191.

Holland, G., Cassidy, M., Ballentine, C.J., 2009. Meteorite Kr in Earth's mantle suggests a late accretionary source for the atmosphere. Science 326, 1522–1525.

Honda, M., McDougall, I., 1998. Primordial helium and neon in the Earth—a speculation on early degassing. Geophys. Res. Lett. 25, 1951–1954.

Honda, M., McDougall, I., Patterson, D.B., Doulgeris, A., Clague, D.A., 1993. Noble gases in submarine pillow basalt glasses from Loihi and Kilauea, Hawaii: a solar component in the Earth. Geochim. Cosmochim. Acta 57, 859–874.

Hudson, G.B., Kennedy, B.M., Podosek, F.A., Hohenberg, C.M., 1989. The early solar system abundance of ^{244}Pu as inferred from the St. Severin chondrite. Lunar Planet. Sci. Conf. Proc. 19, 547–557.

Kendrick, M.A., Scambelluri, M., Honda, M., Phillips, D., 2011. High abundances of noble gas and chlorine delivered to the mantle by serpentinite subduction. Nat. Geosci. 4, 807–812.

Kunz, J., 1999. Is there solar argon in the Earth's mantle? Nature 399, 649–650.

Kunz, J., Staudacher, T., Allègre, C.J., 1998. Plutonium-fission xenon found in Earth's mantle. Science 280, 877–880.

Kurz, M.D., Jenkins, W.J., Hart, S.R., 1982. Helium isotopic systematics of oceanic islands and mantle heterogeneity. Nature 297, 43–47.

Marty, B., 1989. Neon and xenon isotopes in MORB: implications for the earth-atmosphere evolution. Earth Planet. Sci. Lett. 94, 45–56.

Marty, B., Humbert, F., 1997. Nitrogen and argon isotopes in oceanic basalts. Earth Planet. Sci. Lett. 152, 101–112.

Marty, B., Tolstikhin, I.N., 1998. CO_2 fluxes from mid-ocean ridges, arcs and plumes. Chem. Geol. 145, 233–248.

Moreira, M., Escartin, J., Gayer, E., Hamelin, C., Bézos, A., Guillon, F., Cannat, M., 2011. Rare gas systematics on Lucky Strike basalts (37°N, North Atlantic): evidence for efficient homogenization in a long-lived magma chamber system? Geophys. Res. Lett. 38.

Moreira, M., Kunz, J., Allegre, C., 1998. Rare gas systematics in popping rock: isotopic and elemental compositions in the upper mantle. Science 279, 1178–1181.

Moreira, M., Raquin, A., 2007. The origin of rare gases on Earth: the noble gas "subduction barrier" revisited. C. R. Geosci. 339, 937–945.

Mukhopadhyay, S., 2012. Early differentiation and volatile accretion recorded in deep-mantle neon and xenon. Nature 486, 101–104.

Ozima, M., Igarashi, G., 2000. The primordial noble gases in the Earth: a key constraint on Earth evolution models. Earth Planet. Sci. Lett. 176, 219–232.

Ozima, M., Podosek, F.A., Igarashi, G., 1985. Terrestrial xenon isotope constraints on the early history of the Earth. Nature 315, 471–474.

Parai, R., Mukhopadhyay, S., Lassiter, J.C., 2009. New constraints on the HIMU mantle from neon and helium isotopic compositions of basalts from the Cook–Austral Islands. Earth Planet. Sci. Lett. 277, 253–261.

Pepin, R.O., 1991. On the origin and early evolution of terrestrial planet atmospheres and meteoritic volatiles. Icarus 92, 2–79.

Pepin, R.O., 2000. On the isotopic composition of primordial xenon in terrestrial planet atmospheres. Space Sci. Rev. 92, 371–395.

Pepin, R.O., Becker, R.H., Rider, P.E., 1995. Xenon and krypton isotopes in extraterrestrial regolith soils and in the solar wind. Geochim. Cosmochim. Acta 59, 4997–5022.

Pepin, R.O., Porcelli, D., 2006. Xenon isotope systematics, giant impacts, and mantle degassing on the early Earth. Earth Planet. Sci. Lett. 250, 470–485.

Porcelli, D., Wasserburg, G.J., 1995. Mass transfer of helium, neon, argon, and xenon through a steady-state upper mantle. Geochim. Cosmochim. Acta 59, 4921–4937.

Porcelli, D., Ballentine, C.J., Wieler, R., 2002. An overview of noble gas geochemistry and cosmochemistry. Rev. Mineral. Geochem. 47, 1.

Pujol, M., Marty, B., Burgess, R., 2011. Chondritic-like xenon trapped in Archean rocks: a possible signature of the ancient atmosphere. Earth Planet. Sci. Lett. 308, 298–306.

Raquin, A., Moreira, M., 2009. Atmospheric ^{38}Ar/^{36}Ar in the mantle: implications for the nature of the terrestrial parent bodies. Earth Planet. Sci. Lett. 287, 551–558.

Raquin, A., Moreira, M.A., Guillon, F., 2008. He, Ne and Ar systematics in single vesicles: mantle isotopic ratios and origin of the air component in basaltic glasses. Earth Planet. Sci. Lett. 274, 142–150.

Sarda, P., Moreira, M., Staudacher, T., 1999. Argon–lead isotopic correlation in Mid-Atlantic Ridge basalts. Science 283, 666–668.

Sarda, P., Staudacher, T., Allègre, C.J., 1988. Neon isotopes in submarine basalts. Earth Planet. Sci. Lett. 91, 73–88.

Schilling, J.-G., Hanan, B.B., McCully, B., Kingsley, R.H., Fontignie, D., 1994. Influence of the Sierra-Leone Mantle Plume on the Equatorial Mid-Atlantic Ridge: a Nd–Sr–Pb isotopic study. J. Geophys. Res.—Solid Earth 99, 12005–12028.

Schilling, J.-G., Ruppel, C., Davis, A.N., McCully, B., Tighe, S.A., Kingsley, R.H., Lin, J., 1995. Thermal structure of the mantle beneath the Equatorial Mid-Atlantic Ridge: inferences from the spatial variation of dredged basalt glass compositions. J. Geophys. Res.—Solid Earth 100, 10057–10076.

Sumino, H., Burgess, R., Mizukami, T., Wallis, S.R., Holland, G., Ballentine, C.J., 2010. Seawater-derived noble gases and halogens preserved in exhumed mantle wedge peridotite. Earth Planet. Sci. Lett. 294, 163–172.

Tolstikhin, I., Hofmann, A.W., 2005. Early crust on top of the Earth's core. Phys. Earth Planet. Inter. 148, 109–130.

Tolstikhin, I.N., O'Nions, R.K., 1996. Some comments on isotopic structure of terrestrial xenon. Chem. Geol. 129, 185–199.

Trieloff, M., Kunz, J., 2005. Isotope systematics of noble gases in the Earth's mantle: possible sources of primordial isotopes and implications for mantle structure. Phys. Earth Planet. Inter. 148, 13–38.

Trieloff, M., Kunz, J., Allègre, C.J., 2002. Noble gas systematics of the Réunion mantle plume source and the origin of primordial noble gases in Earth's mantle. Earth Planet. Sci. Lett. 200, 297–313.

Trieloff, M., Kunz, J., Clague, D.A., Harrison, D., Allègre, C.J., 2000. The nature of pristine noble gases in mantle plumes. Science 288, 1036–1038.

Valbracht, P.J., Staudacher, T., Malahoff, A., Allègre, C.J., 1997. Noble gas systematics of deep rift zone glasses from Loihi Seamount, Hawaii. Earth Planet. Sci. Lett. 150, 399–411.

Wieler, R., Baur, H., 1994. Krypton and xenon from the solar wind and solar energetic particles in two lunar ilmenites of different antiquity. Meteoritics 29, 570–580.

Workman, R.K., Hart, S.R., 2005. Major and trace element composition of the depleted MORB mantle (DMM). Earth Planet. Sci. Lett. 231, 53–72.

Yokochi, R., Marty, B., 2004. A determination of the neon isotopic composition of the deep mantle. Earth Planet. Sci. Lett. 225, 77–88.

Yokochi, R., Marty, B., 2005. Geochemical constraints on mantle dynamics in the Hadean. Earth Planet. Sci. Lett. 238, 17–30.